The Plant Cell, Vol. 5, 25–38, January 1993

RESEARCH ARTICLE

Endoplasmic Reticulum Forms a Dynamic Continuum for Lipid Diffusion between Contiguous Soybean Root Cells

Sharon Grabski,[a] Adriaan W. de Feijter,[b] and Melvin Schindler [a,1]

[a] Department of Biochemistry, Michigan State University, East Lansing, Michigan 48824
[b] Meridian Instruments, 2310 Science Parkway, Okemos, Michigan 48864

Intercellular communication between plant cells for low molecular weight hydrophilic molecules occurs through plasmodesmata. These tubular structures are embedded in the plant cell wall in association with the plasmalemma and endoplasmic reticulum (ER). Transmission electron microscopy has provided strong evidence to support the view that both the ER and plasmalemma are structurally continuous across the wall at these sites. In experiments to be described, the technique of fluorescence redistribution after photobleaching was used to examine the lateral mobility and intercellular transport capability of a number of fluorescent lipid and phospholipid analogs. These probes were shown by confocal fluorescence microscopy to partition in either the ER or plasmalemma. Results from these measurements provide evidence for cell communication between contiguous cells for probes localized predominantly in the ER. In contrast, no detectable intercellular communication was observed for probes residing exclusively in the plasmalemma. It was of particular interest to note that when 1-acyl-2-(*N*-4-nitrobenzo-2-oxa-1,3-diazole)aminoacylphosphatidylcholine was utilized as a potential reporter molecule for phospholipids in the plasmalemma, it was quickly degraded to 1-acyl-2-(*N*-4-nitrobenzo-2-oxa-1,3-diazole)aminoacyldiglyceride (NBD-DAG), which then appeared predominantly localized to the ER and nuclear envelope. This endogenously synthesized NBD-DAG was found to be capable of transfer between cells, as was exogenously incorporated NBD-DAG. Results from these investigations provide support for the following conclusions: (1) ER, but apparently not the plasmalemma, can form dynamic communication pathways for lipids across the cell wall between connecting plant cells; (2) the plasmodesmata appear to form a barrier for lipid diffusion through the plasmalemma; and (3) lipid signaling molecules such as diacylglycerol are capable of transfer between contiguous plant cells through the ER. These observations speak to issues of plant cell autonomy for lipid synthesis and mechanisms of intercellular signaling and communication.

INTRODUCTION

Morphological evidence to date suggests that plasmodesmata, the tubular structures connecting the cytoplasmic compartments of contiguous plant cells, are in association with the plasmalemma in the cell wall (Robards, 1976). Incorporated within this plasmalemma-delimited gap is the dominant transwall structural component of plasmodesmata called the desmotubule (Robards, 1976). Considerable efforts utilizing transmission electron microscopy have been dedicated to elucidating the structure and composition of the desmotubule (Lopez-Saez et al., 1966; Robards, 1968; Overall et al., 1982; Robards and Lucas, 1990), but as pointed out by Tilney et al. (1991), the interpretations of structure "have changed repeatedly backwards and forwards." Suggestions for organization have varied between descriptions of a lipid-containing tubule connected to endoplasmic reticulum (ER) (Lopez-Saez et al., 1966; Overall et al., 1982) to the structure of a microtubule-like rod composed of protein subunits (Robards, 1968). Difficulties in the interpretation of transmission electron microscopy images have been ascribed to the relatively small size of the structure, the inability to isolate plasmodesmata from plant tissue, and the "Draconian" methods available to microscopists (Tilney et al., 1991). Interpretations of plasmodesmatal structure and organization that are solely dependent on transmission electron microscopy images must, therefore, be considered with caution. Within the constraints of this caveat, it does appear that sufficient data exist to support the view that both plasmalemma and ER traverse the cell wall at the sites of plasmodesmata insertion (Robards, 1976; Robards and Lucas, 1990; Tilney et al., 1991).

To examine the dynamic consequences of these observed membrane continuities between cells, Baron-Epel et al. (1988) set out to pursue the possibility that the plasmalemma might serve as a membrane communication pathway for the migration

[1] To whom correspondence should be addressed.

of lipid/phospholipid molecules between cells. 1-Acyl-2-(*N*-4-nitrobenzo-2-oxa-1,3-diazole)aminoacylphosphatidylcholine (NBD-PC) was utilized as a phospholipid analog to characterize the potential continuity between contacting cells. The results of those experiments were interpreted to provide evidence for a membrane communication pathway between cells across the cell wall.

In an effort to further explore these original observations, we have utilized additional fluorescent lipid and phospholipid analogs that have been shown by confocal fluorescence microscopy to partition predominantly in either the ER or plasmalemma. The results of these experiments provide strong support for the proposal that the ER may serve as a diffusion pathway for lipid molecules between contiguous cells. In contrast, probes that are localized to the plasmalemma may diffuse within the plane of the membrane of an individual cell, but appear incapable of crossing between cells. These experiments also showed that NBD-PC exogenously added to soybean root cells is rapidly converted to 1-acyl-2-(*N*-4-nitrobenzo-2-oxa-1,3-diazole)aminoacyldiglyceride (NBD-DAG), a fluorescent analog of the second messenger of the phosphatidylinositol signaling pathway, diacylglycerol (Berridge, 1984). The resultant product, NBD-DAG, is found to translocate to the ER and may then diffuse across the cell wall to contiguous cells. These observations, in toto, provide evidence that the ER can serve as a dynamic pathway for the movement of lipids and lipid-signaling molecules.

RESULTS

Endomembrane Probes—Localization of Cellular Fluorescence

Fluorescent lipid and phospholipid analogs were utilized to examine potential plasmalemma- and endomembrane-mediated communication between contiguous soybean root cells. Confocal microscopy (Shotten, 1989) was used to provide a detailed view of the fluorescence distribution for these probes. Both 3,3′-dihexyloxacarbocyanine [$DiOC_6(3)$] and rhodamine B hexyl ester have been previously shown to label identical endomembrane compartments in animal cells (Terasaki and Reese, 1992). As shown in the confocal micrographs in Figure 1, this labeling similarity is also observed in soybean root cells. ER, mitochondria, and lipid bodies are labeled by these two stains. As shown in Figure 1A, there are a variety of morphologies observed for the ER. Both a tubular polygonal network and cisternal form are apparent (Quader et al., 1989; Hepler et al., 1990). In addition, a long, snaking rodlike structure (Figure 1A, arrow) is seen that is close to or in association with the tubular and cisternal forms. Closer views of these three types of endomembrane (all of these types presumably ER as defined in Hepler et al., 1990) are presented in Figure 2. Because of the enhanced photostability observed for rhodamine B hexyl ester, all further staining and imaging of the ER was performed with this fluorescent lipophilic probe.

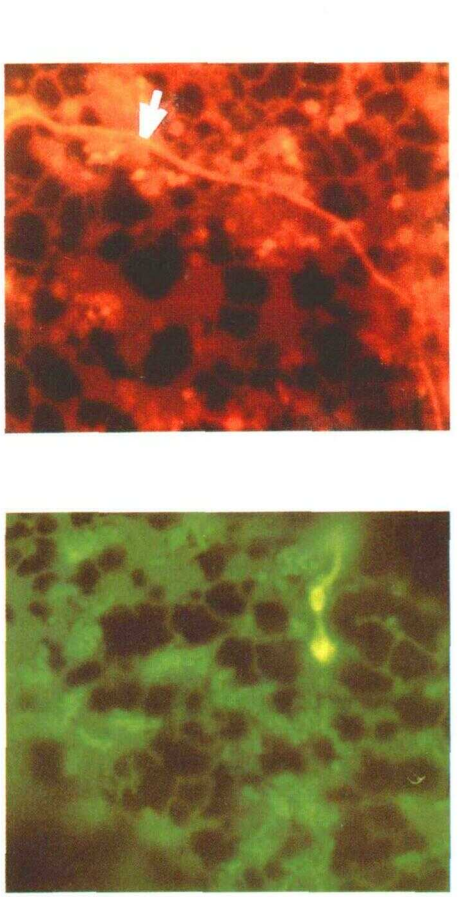

Figure 1. Fluorescent Images of the Endomembranes in Soybean Root Cells Stained with $DiOC_6(3)$ and Rhodamine B Hexyl Ester.

Soybean cultivar Mandarin root cells (SB-1 cell line) were grown in suspension culture and stained as described in Methods. Confocal images were obtained with an Insight Bilateral Scanning Confocal Microscope as described in Methods.

(A) Endomembranes of cells labeled with rhodamine B hexyl ester. The arrow denotes the snaking rodlike ER.

(B) Sample stained with $DiOC_6(3)$.

Images are 6000×.

Figure 2A presents a view of an extensive polygonal tubular network with which a variety of organelles appear to associate, for example, mitochondria and lipid bodies. Figure 2B shows an area of ER containing an abundance of the cisternal type (flat sheets). Single (arrow) and clustered mitochondria (boxed area) are seen to have the same color and intensity of labeling as the ER. Continuous examination of the stained ER in living cells showed that the polygonal tubular network could convert into the cisternal form, apparently by swelling

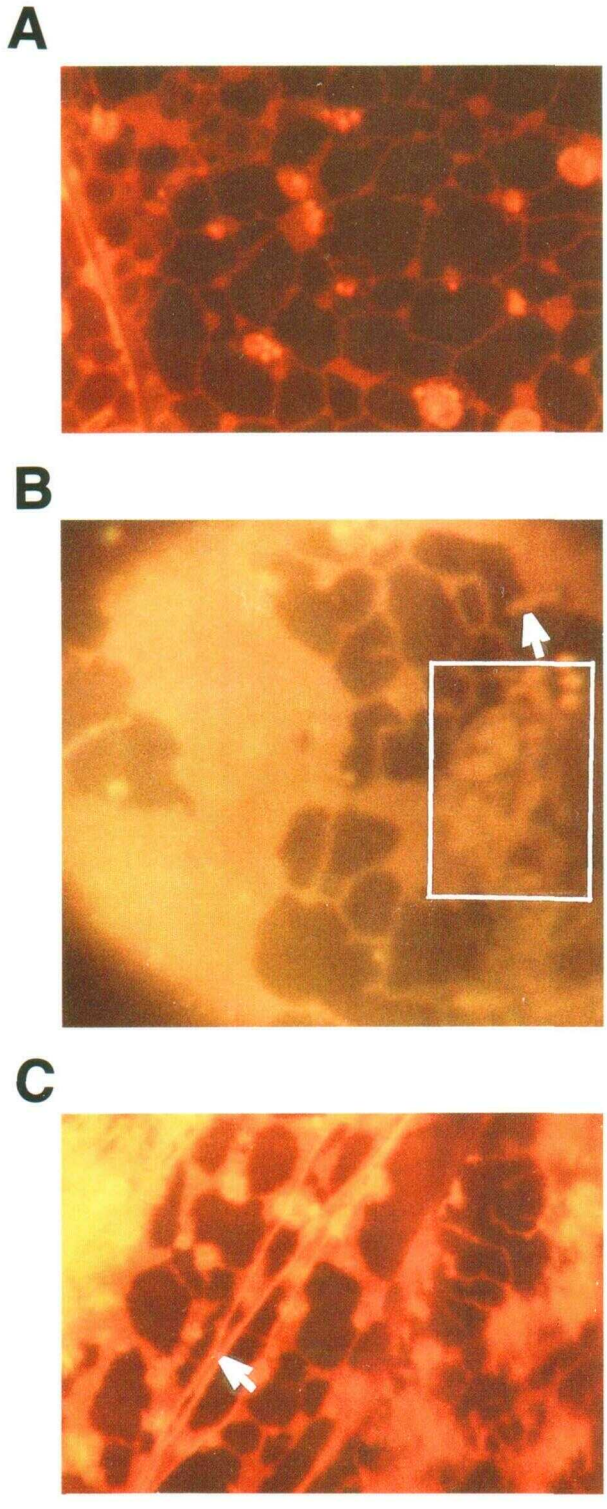

Figure 2. Structural Variability of ER in Soybean Root Cells.

Rhodamine B hexyl ester staining of soybean root cells shows three types of ER.

(A) Tubular polygonal reticulum.

(B) Flat cisternal strands.

(C) Snaking rodlike strands.

Mitochondria and lipid bodies are found close to the endomembranes and appear to associate with them. **(B)** Shows a single mitochondrion (arrow) and a cluster of mitochondria (box) localized to a cisternal surface. Images in **(A)** and **(C)** are 6000× and in **(B)**, 9000×.

and fusion, as previously noted by Quader et al. (1989). In Figure 2C, the long, snaking rodlike forms of ER (arrow) may be observed within the same focal plane as the tubular and cisternal forms of ER.

As shown in Figure 3, a series of fluorescent sections at different planes of focus through a soybean cell are simultaneously observed with a phase view of the soybean cell. In the image shown in Figure 3A, the fluorescent view is of the focal plane closest to the cell wall. This cell surface is in contact with the coverslip. As the focus moves through the cell (Figures 3B and 3C) from a position closest to the objective of an inverted microscope, transcytoplasmic strands, nuclear envelope, and membranes of vesicles positioned around the nucleus show fluorescent labeling. The imaging data support the view that rhodamine B hexyl ester and $DiOC_6(3)$ can label the entire endomembrane system of soybean root cells with varying degrees of intensity as reported for animal cells (Terasaki and Reese, 1992). An additional lipid probe, 5-(*N*-dodecanoylaminofluorescein (AFC_{12}), was found to distribute in a similar fashion in soybean root cells (data not shown).

To specifically examine the intercellular transport competency of the plasmalemma, we initially utilized NBD-PC, a fluorescent phospholipid analog of phosphatidylcholine. We have previously used this probe to measure intercellular communication between membrane compartments (Baron-Epel et al., 1988) and in examinations of phospholipid diffusion in protoplasts (Metcalf et al., 1986). Confocal examination of the cellular distribution of this phospholipid analog demonstrated that, within minutes of addition to the cells, the stain could be found in the same intracellular compartments observed for $DiOC_6(3)$ and rhodamine B hexyl ester, as shown in Figure 4. Intracellular organelles, nuclear envelope, transcytoplasmic strands, and all forms of ER were stained (Figures 4A to 4D). Previous work by Pagano and Longmuir (1985) demonstrated that exogenously incorporated phospholipids can rapidly redistribute to endomembranes following flip–flop from the outer to inner leaflet of the plasma membrane in animal cells. Exogenously supplied NBD-PC, previously demonstrated not to flip–flop, still demonstrated endomembrane labeling (Pagano and Longmuir, 1985). Characterization of the labeled species showed that this probe was metabolized predominantly to NBD-DAG, which could then redistribute throughout the endomembrane compartments.

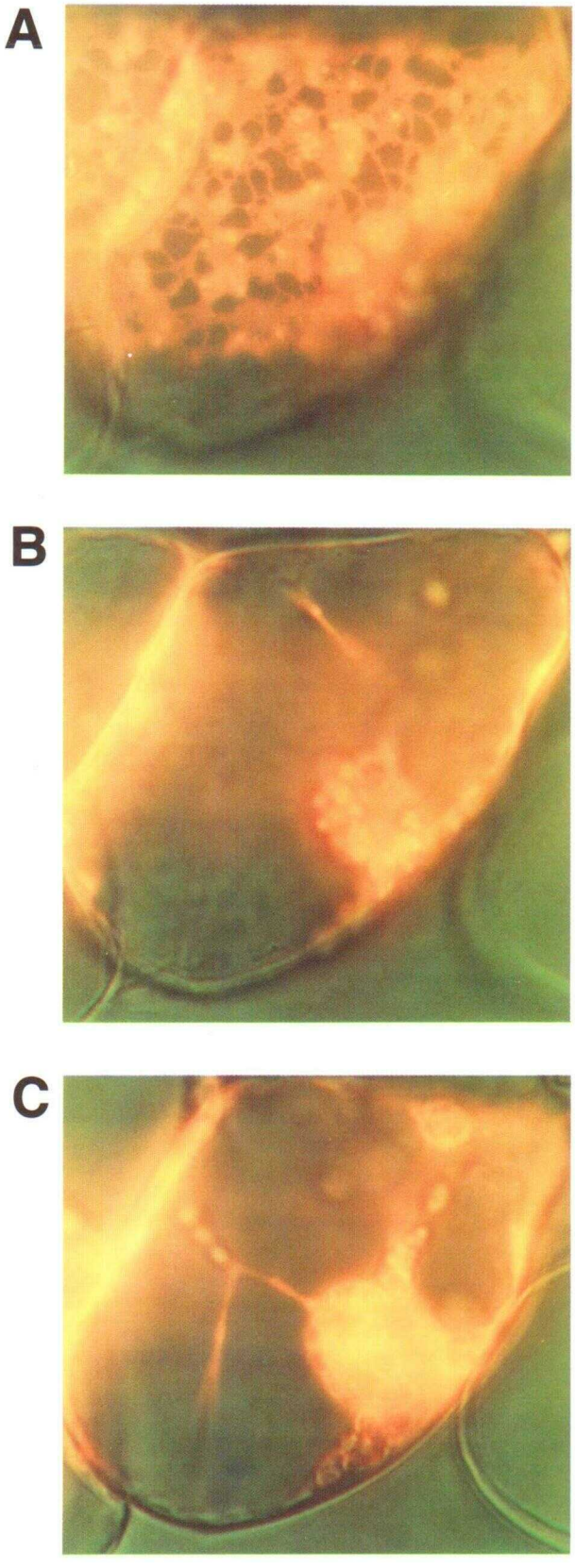

As shown in Figure 5, when a similar chemical analysis was pursued for the fluorescent species in soybean root cells following incorporation of NBD-PC, significant conversion was observed to NBD-DAG (Figure 5, lanes a and b). It is of interest that conversion was higher in cells not prewashed in 1B5C medium (Metcalf et al., 1983) (Figure 5, lane a) than in those cells that had been prewashed (Figure 5, lane b). An analysis of the culture medium of unwashed cells indeed demonstrated hydrolytic activity converting NBD-PC to NBD-DAG (data not shown). This was not observed for fresh media following incubation with prewashed cells for up to an hour. Quantitation of NBD-PC hydrolysis (see Methods) showed that conversion to NBD-DAG was maximal 15 min after the addition of NBD-PC to prewashed cells. Approximately 75 to 80% of the fluorescent label was observed in the product NBD-DAG as quantitated using fluorescence spectrofluorometry as described in Methods. The imaging data, in conjunction with a biochemical analysis of the fluorescing species in the cell, provides evidence that $DiOC_6(3)$, rhodamine B hexyl ester, AFC_{12}, and NBD-DAG all incorporate into endomembrane compartments and may be utilized to examine ER–mediated intercellular communication.

N-(6-(7-nitrobenz-2-oxa-1,3-diazole-4-yl)amino)-hexanoyl)-sphingosylphosphocholine and Nonhydrolyzed NBD-PC as Probes for Plasmalemma Dynamics

Although exogenously incorporated NBD-PC was converted to NBD-DAG within the cell, this conversion could be inhibited if incorporation of NBD-PC was performed in the presence of 2 mM EDTA at 4°C (Figure 5, lane g). Previous reports have suggested a phosphatidylinositol-specific phospholipase C in soybean cells that requires Ca^{2+} for activity (Pfaffmann et al., 1987) with low activity for phosphatidylcholine. The observed conversion may be catalyzed by this enzyme or other types of phospholipase C. Confocal images of the intracellular distribution of NBD-PC incorporated under conditions preventing conversion to NBD-DAG are shown in Figure 6. Diffuse labeling is seen surrounding the nucleus (Figure 6A). This labeling was in contrast to the nuclear and perinuclear vesicle membrane staining observed for the endomembrane probes (Figure 4). Focusing to the cell surface nearest the cell wall showed a diffuse fluorescence with a granular appearance (Figure 6B).

Figure 3. Confocal Fluorescent Sections of Soybean Root Cells Stained with Rhodamine B Hexyl Ester Simultaneously Viewed with Phase Microscopy.

Labeled cells were examined at different focal planes while maintaining phase illumination of the sample.
(A) Image from the surface closest to the cell wall that is in contact with a coverslip.
(B) Image at a medial position.
(C) Image at a focal plane including the nucleus.
Images are 3000×.

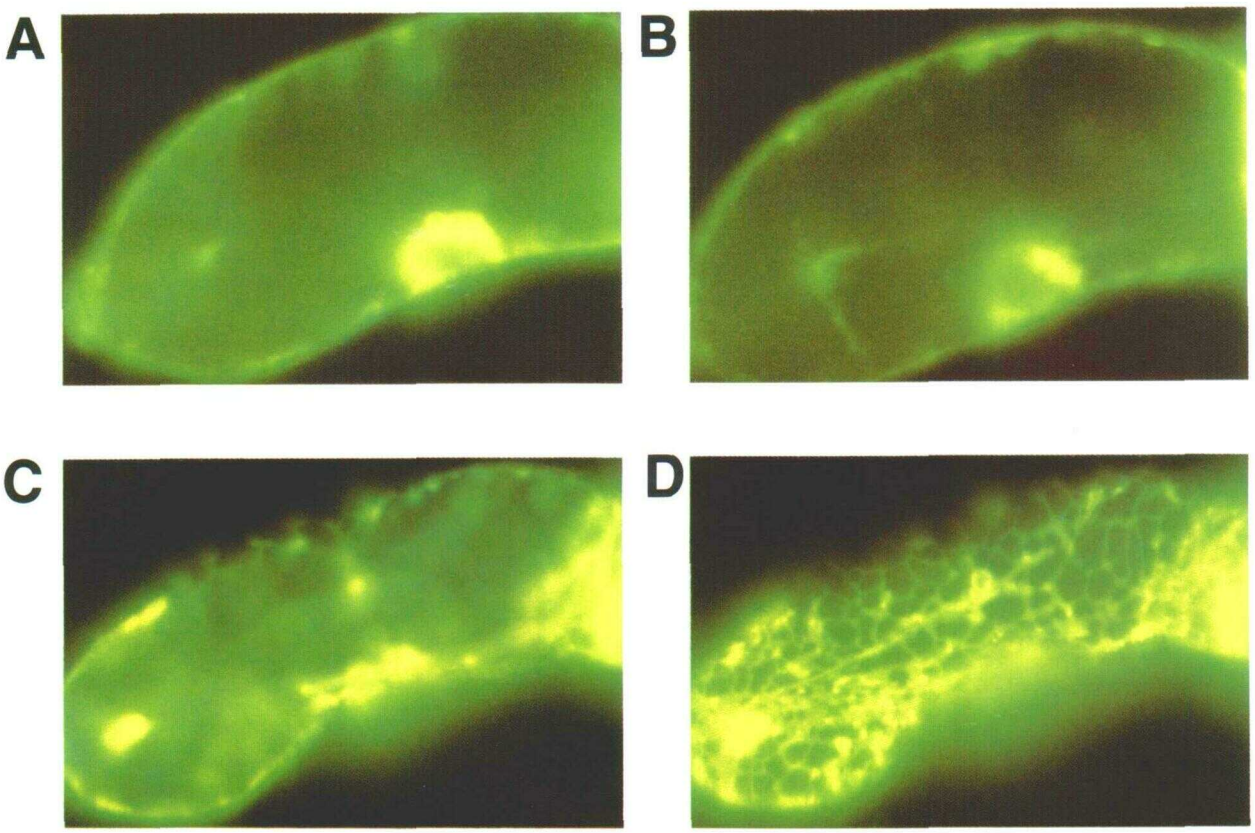

Figure 4. Distribution of Endogenously Produced Metabolic Products of NBD-PC Hydrolysis in Soybean Root Cells.

"Unwashed" cells were labeled with NBD-PC for 20 min at room temperature (incubation at 4°C demonstrated a similar hydrolysis) as described in Methods.

(A) Image of labeled cell at a focal plane including the nucleus.

(B) and **(C)** Intermediate optical sections of the labeled cell.

(D) Membrane organization closest to the cell wall touching the coverslip surface.

Images are 3000×.

This contrasts with images of crisp ER observed for the endomembrane probes (Figures 1 to 4).

To employ a more specific probe for the plasmalemma, *N*-(6-(7-nitrobenz-2-oxa-1,3-diazole-4-yl)amino)hexanoyl)sphingosylphosphocholine (NBD-SM) was exogenously incorporated into cells, and its cellular distribution and biochemical fate were examined. As shown in Figure 5, lane h, NBD-SM monitored in cells at room temperature yielded a small amount of 6-((*N*-(7-nitrobenz-2-oxa-1,3 diazole-4-yl)amino)caproyl)sphingosine (NBD-Cer). This conversion could be prevented if NBD-SM was incorporated and examined in media containing 2 mM EDTA at 4°C (Figure 5, lane i), providing further evidence for a Ca^{2+}-mediated phospholipase C activity. A phase view of these cells is shown in Figure 7A, and a confocal fluorescent image of these cells is presented in Figure 7B. For cells maintained at 4°C in the presence of 2 mM EDTA, the nuclear region showed no fluorescence (Figure 7B) and no staining of the ER or other intracellular organelles. The data support a view that NBD-SM, in the presence of EDTA and maintained at 4°C, is not metabolized or internalized during the course of mobility measurements (~30 min) and resides in the plasmalemma.

Lateral Mobility of Lipids in the Plasma Membrane and ER

Lateral mobility measurements were pursued as an independent approach to examine the membrane properties of fluorescent lipid and phospholipid probes. The technique of fluorescence redistribution after photobleaching (FRAP) was used for these measurements, as previously described (Metcalf et al., 1986). In assessing the diffusion rates shown in Table 1, it is important to note that for probes incorporated into endomembranes, NBD-DAG, AFC_{12}, and $DiOC_6(3)$, the diffusion rates measured should be considered apparent diffusion rates because the measurement beam (~1 μm in diameter) was

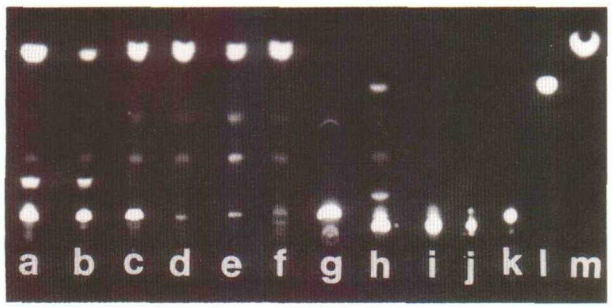

Figure 5. Analysis of Fluorescent Lipid Probe Metabolism in Soybean Root Cells.

Cells were labeled with fluorescent lipid probes and extracted for TLC analysis as described in Methods. Viewing the TLC plates under long-wave UV excitation, NBD-PC hydrolysis to NBD-DAG was observed following 10-min incubation with "unwashed" (see Methods) or "prewashed" cells at 4°C (lanes a and b, respectively). Lanes c to f show exogenously incorporated NBD-DAG in unwashed cells incubated for 2 min at 4°C, NBD-DAG in prewashed cells incubated for 2 min at 4°C, NBD-DAG in unwashed cells incubated for 10 min at 4°C, and NBD-DAG in prewashed cells incubated for 10 min at 4°C, respectively. Lane g contains NBD-PC incubated for 10 min at 4°C in prewashed cells in the presence of 2 mM EDTA. NBD-SM in prewashed cells was incubated for 10 min at 4°C in the absence (lane h) and presence (lane i) of 2 mM EDTA. Standards are NBD-SM (lane j), NBD-PC (lane k), NBD-Cer (lane l), and NBD-DAG (lane m).

focused to a region containing membrane tubules and sheets with intervening spaces rather than a two-dimensional membrane continuum. Table 1 shows that all endomembrane probes have membrane lipid–type diffusion rates, with varying degrees of recovery. NBD-SM and NBD-PC demonstrated diffusion values similar to those previously reported for phospholipid mobility in protoplasts (Metcalf et al., 1986). Measurements of the diffusion of NBD-PC in the presence of 2 mM EDTA at 4°C showed a diffusion rate similar to NBD-SM, but with a significantly larger immobile species. This is consistent with the uptake of NBD-PC into the plasmalemma and subsequent internalization of a large fraction of this probe into intracellular structures, as observed in Figure 6. It would appear that the NBD-PC residing in the internal membrane compartments is not exchangeable over the time course of analysis. It is important to point out that when utilizing the FRAP procedure, it is difficult to distinguish between an immobilized fraction and the existence of small membrane domains (diameter $\leq 2\ \mu m$) of mobile lipid that are not free to exchange across diffusional barriers.

Measurement of Intercellular Communication of Lipids between Contiguous Cells

Diffusion of Lipids between Cells

Soybean root cells labeled as detailed in Methods were subjected to the fluorescence transport assay (Baron-Epel et al., 1988) to examine dynamic continuity for both endomembrane and plasmalemma. As observed in Figures 8A and 8C, the endomembrane probe, $DiOC_6(3)$, can transfer between contiguous cells. The cell areas analyzed are bordered by black lines and are represented by the attached number. The bleached cell (number 1) regains fluorescence intensity, whereas the unbleached contiguous cells lose fluorescence intensity (numbers 2 and 4). All three cells (1, 2, and 4) are included in the area labeled number 3 and represent the total fluorescence analyzed for photobleaching recovery. An

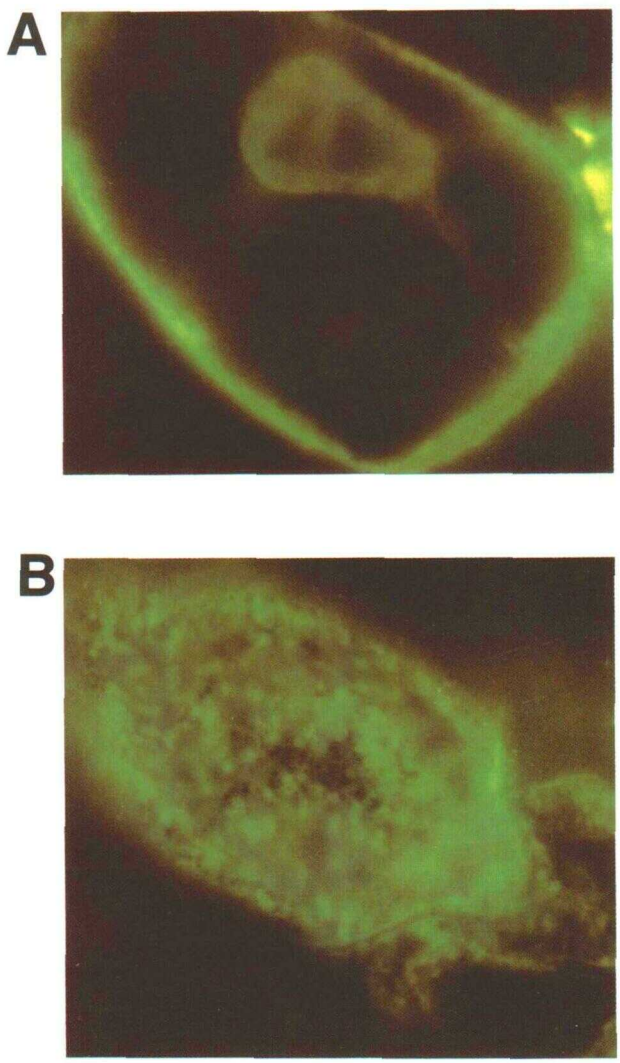

Figure 6. Fluorescence Images of NBD-PC Incorporation into Soybean Root Cells.

Cells were labeled in the presence of 2 mM EDTA at 4°C.
(A) Fluorescent image of an optical section through the nucleus.
(B) Fluorescent image of an optical section at the plasmalemma surface closest to the cell wall in contact with the coverslip surface.
Images are 3000×.

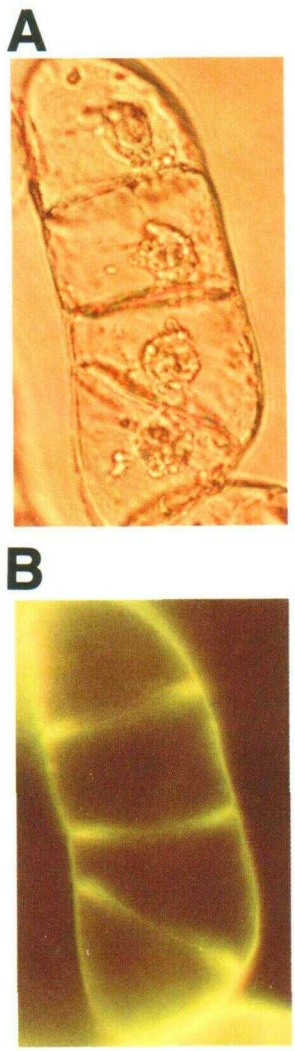

Figure 7. Fluorescence Distribution of NBD-SM in Soybean Root Cells.

Soybean root cells were labeled in the presence of EDTA at 4°C and stained with NBD-SM.

(A) Phase view of NBD-SM–stained cells.

(B) Confocal fluorescent image of NBD-SM–stained cells.

Images are 1100×.

analysis of the fluorescence changes as a function of time is presented in Figure 8D. The numbered curves refer directly to the numbered bordered regions in the images. Curve 1 (green) shows the redistribution of fluorescence to the bleached cell, whereas curves 2 (red) and 4 (dashed black-green) represent the loss of fluorescence from connected cells. Curve 3 (yellow) represents the total fluorescence immediately after photobleaching and is the total fluorescence available for recovery. The extent of fluorescence recovery was found to vary from 50 to 80% for ~40 different experiments.

Figures 8E to 8G show intracellular diffusion within a single cell. Half a cell was photobleached and, as can be observed, there was rapid and apparently complete recovery for the probe throughout the endomembrane system (Figure 8H). This recovery was found to vary between 75 and 100% for 20 samples, and indicates a continuum for $DiOC_6(3)$ diffusion in the endomembrane system. That this continuum is within a membrane phase can be ascertained from the diffusion measurements (Table 1), which demonstrate membrane lipid transport rates and high fluorescence recovery for $DiOC_6(3)$. In Figures 8I through 8K, the consequences of plasmolysis-induced rupture (incubation in 0.7 M sorbitol) of transwall intercellular linkages may be observed. Although no communication is seen for $DiOC_6(3)$ between cells (Figure 8L), intracellular transport still occurs (Figures 8J and 8K), demonstrating that plasmolysis does not alter the endomembrane dynamic continuum within a cell. A similar pattern of inter- and intracellular membrane communication was seen for AFC_{12} and rhodamine B hexyl ester (data not shown). The lack of fluorescence observed in the cell wall of plasmolyzed cells also provides good evidence that the wall does not compartmentalize the endogenously incorporated probes.

Intercellular transport for exogenously incorporated NBD-DAG is shown in Figures 9A to 9D. Numbering for the images (Figures 9A through 9C) and the recovery curves (Figure 9D) is the same as described for Figures 8A through 8D. The extent of recoverable fluorescence for NBD-DAG between cells varied between 30 and 60%. This is not due to significant metabolism of NBD-DAG to other products during the experiment (15 to 30 min) (Figure 5, lanes e and f), but may suggest either a specific subcompartmentalization or sequestration that limits the amount of exchangeable NBD-DAG. Interestingly, analysis of NBD-DAG metabolism following 2 min of incubation revealed the apparent formation of NBD-PC (Figure 5, lanes c and d), which then seems to be hydrolyzed back to NBD-DAG after 10 min (Figure 5, lanes e and f). NBD-DAG was also found to quickly exchange between labeled endomembrane compartments within a single cell, as shown in Figures 9E to 9G. The relatively high recovery observed in Figures 9E to 9H is apparently a consequence of the smaller area of analysis (circle around nuclear region). Plasmolysis, on the other hand,

Table 1. Lateral Diffusion of Fluorescent Lipid and Phospholipid Analogs in Soybean Root Cell Membranes

Probe	D^a ($\times 10^9$ cm²/s ± SD)	R^b (% ± SD)
$DiOC_6(3)$	1.3 ± 0.4[c]	75 ± 10
AFC_{12}	2.0 ± 1.0[c]	66 ± 13
NBD-DAG	2.3 ± 1.4[c]	49 ± 10
NBD-SM	0.18 ± .07[d]	62 ± 10
NBD-PC	0.30 ± .12[d]	30 ± 11

[a] Diffusion coefficients are derived from 20 to 40 independent measurements on different cells.

[b] Percentage of mobile fluorescent probe.

[c] Apparent diffusion rate.

[d] Measured in the presence of 2 mM EDTA at 4°C.

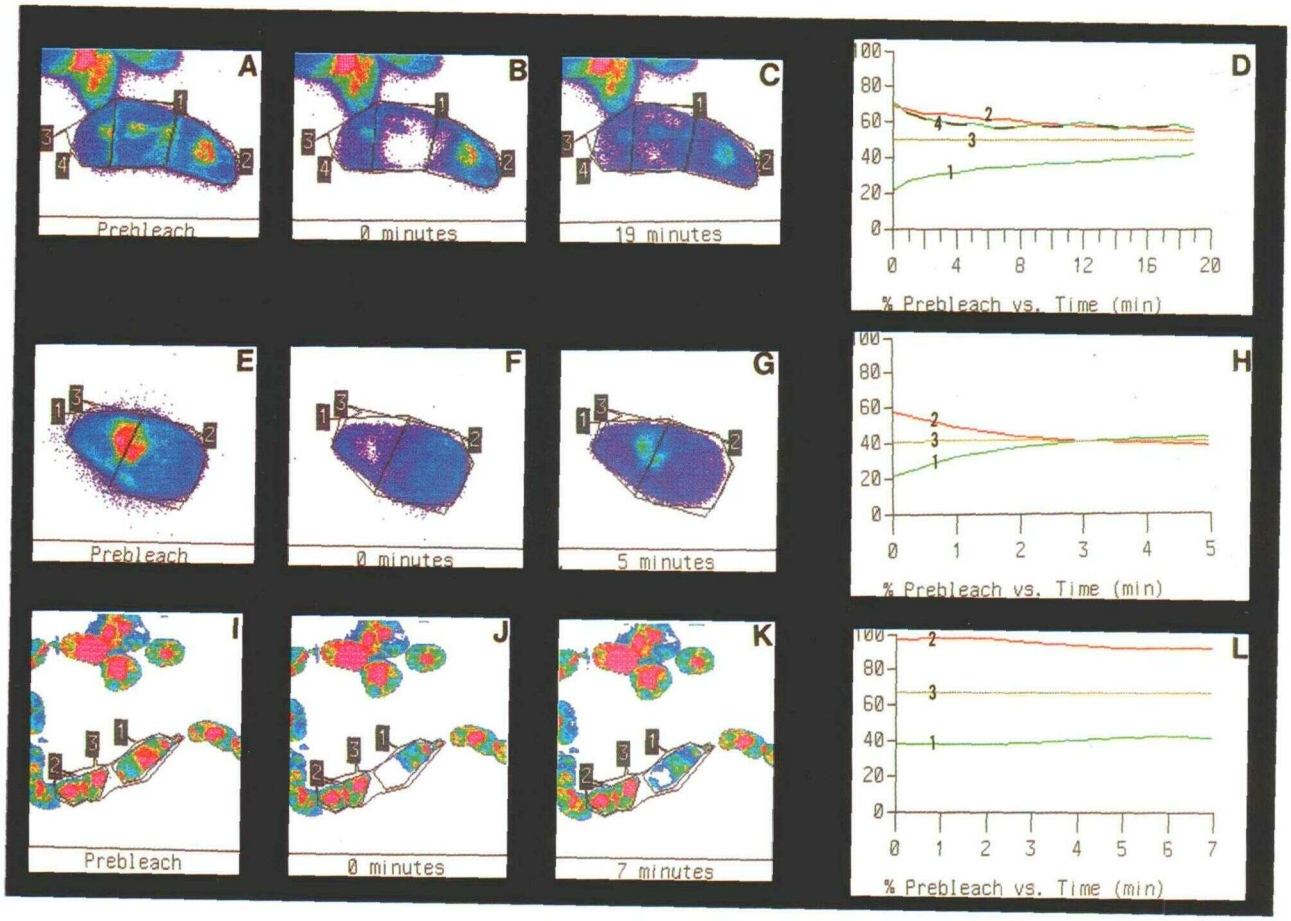

Figure 8. Intercellular Transport as Measured by the Recovery of Fluorescence in Photobleached Soybean Root Cells Stained with $DiOC_6(3)$.

Cells were stained as described in Methods. Prebleach and postbleach representative images are presented. The ordinate of the recovery curves **([D], [H], and [L])** shown for each experiment represents the integrated fluorescence following photobleaching of a boxed region as a percentage of the prebleach fluorescence intensity. The fluorescence intensity represented by curve 3 should be invariant with time during the course of the experiment, and was utilized to provide a correction for photobleaching that occurs as a result of monitoring the cellular fluorescence. In all instances, the numbered curves represent the changes in the fluorescence intensity within the numbered regions in the preceding images. Regions photobleached are numbered 1. Curves 2 and 4 represent the changes in fluorescence intensity in cell regions contiguous to the photobleached cell. Curve 3 represents the postbleach total fluorescence intensity of all cells in the experiment.

(A) Prebleach fluorescence distribution in cells labeled with $DiOC_6(3)$.

(B) Image of fluorescence distribution following photobleaching (time = 0 min).

(C) Image of fluorescence recovery following the specified time.

(D) Recovery curves for $DiOC_6(3)$.

(E) Prebleach image for a single cell labeled with $DiOC_6(3)$.

(F) Postbleach image (time = 0 min) of the cell.

(G) Image of fluorescence recovery in a single cell.

(H) Recovery curves for $DiOC_6(3)$ in a single cell.

(I) Prebleach fluorescence distribution in cells labeled with $DiOC_6(3)$ and then plasmolyzed in media containing 0.7 M sorbitol.

(J) Postbleach image (time = 0 min).

(K) Image of fluorescence recovery for cells.

(L) Recovery curves for $DiOC_6(3)$ in plasmolyzed cells.

Experiments were run until no further recovery was observed. Cells were used up to 1 hr after labeling.

terminated intercellular communication (Figures 9I to 9L). Results for endogenously synthesized NBD-DAG were essentially the same as those reported for exogenously incorporated NBD-DAG.

Diffusion through the Plasmalemma

Although we had initially intended to use NBD-PC as a marker and reporter group for plasmalemma, it became clear after both confocal analysis (Figure 4) and the chromatographic analysis of cells following NBD-PC incorporation (Figure 5) that the original compound was metabolized to NBD-DAG and then found to reside in the internal membrane compartments. To avoid these complications of phospholipid metabolism in whole plant cells, we turned to another fluorescent lipid analog, NBD-SM, which was found to incorporate into the outer leaflet of the plasma membrane in animal cells (Lipsky and Pagano, 1985). We also expected that it might be a poor substrate for either a phosphatidylinositol-specific phospholipase C found in soybean cells (Pfaffmann et al., 1987) or possibly phosphatidylcholine-specific phospholipase C enzymes. As observed in Figure 5, lane h, there was some limited degradation of NBD-SM to NBD-Cer during the course of our analysis, which can be prevented with the addition of 2 mM EDTA (Figure 5, lane i). In addition, confocal microscopy clearly shows peripheral labeling and no nuclear or endomembrane fluorescence (Figure 7) in the presence of 2 mM EDTA at 4°C. As also noted in Table 1, fluorescence recovery data suggests a large mobile species. These results may be interpreted to suggest that

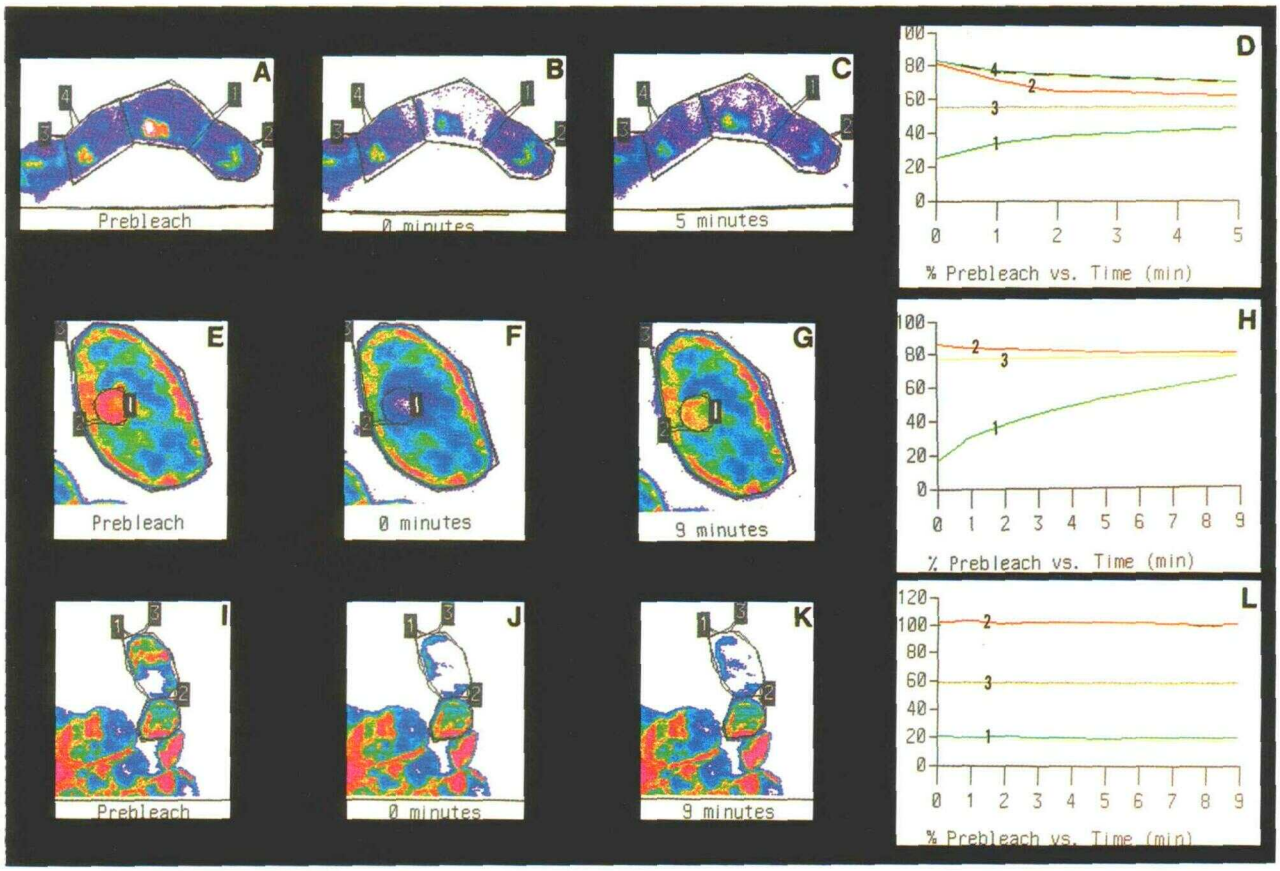

Figure 9. Recovery of Fluorescence in Photobleached Soybean Root Cells Stained with NBD-DAG.

Cells were labeled with NBD-DAG as described in Methods. Numbered regions and curves are as described in Figure 8.
(A) to **(C)** Photobleaching experiment for cells exogenously labeled with NBD-DAG.
(D) Recovery curves for **(A)** to **(C)**.
(E) to **(G)** Experiments for a single cell labeled with NBD-DAG.
(H) Recovery curves for **(E)** to **(G)**.
(I) to **(K)** Photobleaching experiment with plasmolyzed cells labeled with NBD-DAG.
(L) Recovery curves for **(I)** to **(K)**.

NBD-SM is localized to the plasmalemma and can be utilized as a probe for examining intercellular dynamic continuity for the plasmalemma between contiguous cells.

As shown in Figures 10A through 10D, no intercellular communication is observed for NBD-SM incubated in the presence of EDTA at 4°C. This is in contrast to intracellular transport, which is observed for the plasmalemma localized NBD-SM within a single cell (Figures 10E to 10H). Because incorporation of NBD-PC in the presence of 2 mM EDTA at 4°C inhibited conversion of NBD-PC to NBD-DAG (Figure 5, lane g), we utilized this approach to specifically maintain NBD-PC in an unmetabolized form in the plasmalemma. As observed in the confocal image presented in Figure 6, NBD-PC could still enter the cells in a nondegraded form. Although no longer found in a distinct ER, it appeared to be captured in vesicular structures containing lipids (Figure 6B). The significant immobile/sequestered fraction observed following photobleaching in the presence of EDTA (Table 1) supports the interpretation of an internal pool of nonexchangeable labeled lipid, presumably derived from the plasmalemma. Measurements of intercellular

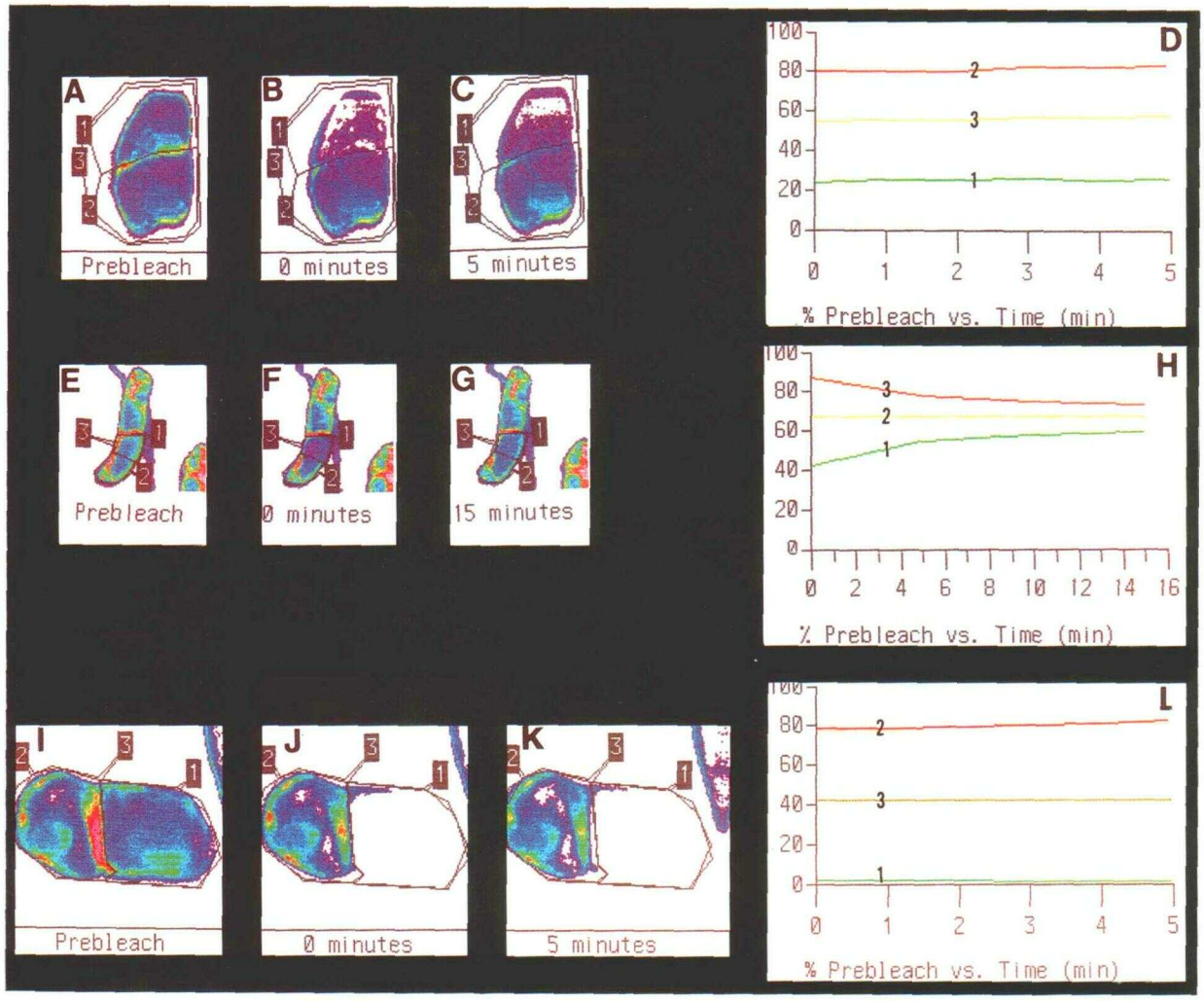

Figure 10. Recovery of Fluorescence in Photobleached Soybean Root Cells Stained with NBD-SM and NBD-PC.

Cells were labeled with both probes as described in Methods. Numbered regions and curves are as described in Figure 8.
(A) to **(C)** Photobleaching experiment for cells labeled with NBD-SM.
(D) Recovery curves for **(A)** to **(C)**.
(E) to **(G)** Photobleaching experiment within a single cell.
(H) Recovery curves for **(E)** to **(G)**.
(I) to **(K)** Photobleaching experiment for cells labeled with NBD-PC.
(L) Recovery curves for **(I)** to **(K)**.
Measurements were performed in the presence of 2 mM EDTA at 4°C.

diffusion for NBD-PC in the presence of 2 mM EDTA at 4°C (note peripheral staining) demonstrated no communication (Figures 10I to 10L), suggesting that ~30% of the mobile fluorescent species (Table 1) is also prevented from partitioning between cells.

DISCUSSION

Although numerous attempts have been made to examine plasmodesmata utilizing electron microscopy, the structure and composition of the desmotubule, the rodlike and most recognizable element of plasmodesmata, are still not resolved. A consensus appears to exist that the desmotubule is connected to the ER. Lopez-Saez et al. (1966) and Overall et al. (1982) postulated that the desmotubule comprises a membrane channel composed of strands of ER threading through the cell wall at sites of plasmodesmata insertion, whereas a recent model proposed by Tilney et al. (1991) suggests a protein-rich rod that resembles a cytoskeletal element. Inherent in the lipid tubule model (Lopez-Saez et al., 1966; Overall et al., 1982) is the idea of a physical continuity of ER membrane between cells, suggesting a potential pathway for lipophilic molecules and possibly membrane-associated proteins. Utilizing the techniques of confocal microscopy and FRAP, an effort was initiated to test whether lipids and/or phospholipids were capable of membrane-mediated diffusion across the cell wall barrier between cells, and whether such a possible transport pathway was mediated by the plasmalemma, the ER, or both.

Considering previous reports of the utility of $DiOC_6(3)$ as a probe for the ER (Terasaki et al., 1984; Quader and Schnepf, 1986), our confocal images clearly show that all endomembranes were labeled by this probe. Because the ER clearly represents the most continuous and connected endomembrane system within the cell, and transmission electron micrographs of plasmodesmata clearly show the ER as the unique endomembrane traversing the cell wall, we interpret our photobleaching results as providing dynamic evidence that $DiOC_6(3)$ is capable of diffusion-mediated transfer between cells by means of the ER. Evidence to support a membrane pathway for this diffusion is threefold: (1) the rate of transfer is slower than previously reported rates for cytoplasmic communication (Baron-Epel et al., 1988); (2) the diffusion rate measured for lipid probes in endomembranes is three to four orders of magnitude slower than aqueous diffusion; and (3) membrane continuity between cells is required for cell-to-cell transfer to occur (plasmolysis prevents communication). It also appears likely that the intracellular membrane continuum observed for the ER is capable of mediating rapid lipid diffusion throughout the intracellular volume. In addition, our results may be interpreted to suggest that lipids can transfer between endomembrane compartments, for example, mitochondria and ER, by means of diffusion between contacting membranes. Confocal images provide evidence for direct contact between endomembrane compartments, such as ER, mitochondria, and lipid bodies. Such contact may be sufficient for collision-mediated transfer of phospholipids between organelles as discussed for the ER and mitochondria in animal cells (Vance, 1990a, 1990b).

Our data, in conjunction with other reports, present evidence that lipids and phospholipids are capable of diffusion-mediated exchange between endomembrane compartments within a cell and across the cell wall. That these observations are not unique to $DiOC_6(3)$ was demonstrated by similar results obtained with a fluorescent fatty acid analog, AFC_{12} (a fatty acid fluorescein amide) and the fluorescent analog of diacylglycerol, NBD-DAG. Both probes showed endomembrane localization and similar intercellular transport kinetics. The lower intercellular recovery rates for NBD-DAG may suggest specific sequestration or compartmentalization for this important molecule which serves as both a metabolic intermediate of phospholipid biosynthesis (Somerville and Browse, 1991) and second messenger involved in cell signaling events in animal cells (Berridge, 1984).

In our initial examination of membrane-mediated communication between cells, we utilized the probe NBD-PC as a reporter molecule (Baron-Epel et al., 1988). It is now clear that upon the addition of NBD-PC to the plasmalemma, it is rapidly converted to NBD-DAG. This presumably occurs as a result of a plasmalemma-localized phospholipase C, whose activity is inhibited by EDTA. Previous reports provide evidence that plant membranes contain a calcium-dependent phosphatidylinositol-specific phospholipase C, demonstrating some activity on phosphatidylcholine (Pfaffmann et al., 1987; Tate et al., 1989). Whether this enzyme is involved in the observed hydrolysis of NBD-PC in soybean cells remains to be determined. However, it should now be considered possible that plant cells can also transduce signals through the turnover of phosphatidylcholine to generate second messengers, such as diacylglycerol and linolenic acid (a precursor of the plant signaling molecule, methyl jasmonate) (Farmer et al., 1992; Gundlach et al., 1992). This would be analogous to the phosphatidylcholine cycles observed in animal cells (Pelech and Vance, 1989; Exton, 1990). This is suggested by our observation that a fraction of exogenously incorporated NBD-DAG can be converted to NBD-PC, which is then metabolized to NBD-DAG. Plants, however, would have the additional signaling capability in that individual cells could either initiate signals for systemic transmission or couple their signaling cycles across plasmodesmata. Another aspect of these results is that they may reflect a plasmalemma-localized degradative pathway that serves as an element of a membrane recycling pathway to remove excess phospholipid from the membrane. Such a proposal has been previously discussed by Staehelin and Chapman (1987).

Plasmalemma-Mediated Intercellular Communication

Transmission electron micrographs of plasmodesmata show that at insertion sites the plasmalemma is structurally continuous across the cell wall. It was somewhat surprising, therefore,

to observe that, although NBD-SM is free to diffuse within the plasmalemma of a cell, this lipid probe is incapable of intercellular transport. In animal cells, such a barrier was reported for lipid diffusion through the region of the plasma membrane forming tight junctions (Dragsten et al., 1981). The possibility exists that the association of the plasmalemma with the plasmodesmata requires protein–protein interactions analogous to those observed at tight junctions. Such interactions might serve in a similar fashion to prevent leakage of cytoplasmic components around the plasmodesmata. These putative anchoring elements could conceivably serve as targets of plant viral disruption, providing a "leakage" pathway for viral transmission between plant cells. A testable prediction of this observation is that the lipids in the plasmalemma of virally infected cells whose plasmodesmata are altered in structure and function (Robards and Lucas, 1990) may transfer intercellularly. This remains to be determined. Although the data with NBD-PC are more complicated to interpret, NBD-PC, in the presence of 2 mM EDTA, is not metabolized and shows both plasmalemma and intracellular localization which presumably occurs as a result of membrane turnover and internalization through endocytosis. The evidence from lateral diffusion measurements (done within 30 min of incorporation at 4°C) suggests that at least 30% of the fluorescent phospholipid analog is free to diffuse, presumably in the plasmalemma. Yet, no intercellular communication is observed for this fraction, supporting the view that the plasmalemma, in association with plasmodesmata, forms a barrier for the diffusion of lipids anchored in the external monolayer of the membrane.

The data presented in our study provide the basis for the following general conclusions: (1) a functional dynamic endomembrane continuum exists within cells and between contiguous cells for the intercellular diffusion of lipids, fatty acids, and the lipid second messenger, diacylglycerol; and (2) a diffusion barrier appears to exist in the plasmalemma at its site of association with the plasmodesmata that prevents the exchange of phospholipids (presumably localized to the outer monolayer) between cells. These results may now provide a context for future investigations to determine the function and role of a dynamic endomembrane continuum between plant cells for mechanisms of plant hormone signal transmission, signal transduction through components of phospholipid metabolism, viral propagation, and pathogenic/symbiotic responses.

METHODS

Labeling of Cells

Communication experiments were performed with soybean (*Glycine max* cv Mandarin) root cells (SB-1 cell line) grown in 1B5C medium (Metcalf et al. 1983) in suspension culture. After 72 to 96 hr of growth, cells were washed three times with the medium 1B5C and incubated with the fluorescent probes at the concentrations given below for varying times, as indicated in the text, at either 4°C or room temperature. These cells are termed "prewashed" cells. In some instances, cells were not prewashed and were used while maintained in the aged growth media. These are defined as "unwashed" cells. Following incubation with fluorescent probe, the cells maintained at the appropriate temperature were again washed three times with media to remove unincorporated dye. The probes used were 3,3'-dihexyloxacarbocyanine [$DiOC_6(3)$] (1 μg/mL); rhodamine B hexyl ester (1 μg/mL); 6-((*N*-(7-nitrobenz-2-oxa-1,3-diazol-4-yl)amino)caproyl) sphingosine (NBD-Cer) (2 μg/mL); *N*-(6-(7-nitrobenz-2-oxa-1,3-diazol-4-yl)amino)hexanoyl)-sphingosylphosphocholine (NBD-SM) (2 μg/mL); and 5-(*N*-dodecanoylamino-fluorescein) (AFC_{12}) (2 μg/mL), which were all obtained from Molecular Probes, Inc. (Eugene, OR). Labeling with 1-acyl-2-(*N*-4-nitrobenzo-2-oxa-1,3-diazole)aminoacylphosphatidylcholine (NBD-PC) obtained from Avanti Biochemicals (Birmingham, AL) (40 μg/mL) was performed both as described above and in the presence of 1B5C containing 2 mM EDTA at 4°C. Inclusion of EDTA was found to significantly inhibit the conversion of NBD-PC to 1-acyl-2-(*N*-4-nitrobenzo-2-oxa-1,3-diazole)aminoacyldiglyceride (NBD-DAG).

Preparation of NBD-DAG

NBD-PC (40 μg/mL) was added to unwashed soybean root cells in 1B5C medium and maintained for 10 min at room temperature. Cells were then centrifuged (400*g* for 5 min) and the lipid was extracted from the cell pellet as previously described (Osborn et al., 1972). The extract was taken to dryness and solubilized in chloroform/methanol (2:1 v/v) (0.25 to 0.5 mL). A series of samples (20 μL) was then applied to a preparative thin-layer chromatography (TLC) plate (DC-Alufolien, Kieselgel-60 F_{254}, 0.2 mm thick [E. Merck, Darmstadt]) and chromatographed in chloroform/methanol/H_2O (65:25:4 v/v) as described previously (Uster and Pagano, 1986). NBD-DAG was identified by comparison of its mobility to a standard (Uster and Pagano, 1986). The fluorescent spot containing the NBD-DAG was scraped from the plate, and the NBD-DAG was eluted from the silica by washing four times with chloroform/methanol (2:1). The silica suspension was centrifuged at 400*g* for 5 min, and the supernatant was evaporated under N_2 and the NBD-DAG was redissolved in ethanol and then stored at −80°C.

Quantitation of Fluorescent Products from TLC Plates

NBD fluorescent spots were scraped from TLC plates and extracted with 2 mL of chloroform/methanol (2:1). The silica suspension was sonicated in a Branson Bath Sonifier for 30 sec and then centrifuged for 2 min at 400*g*. The chloroform/methanol supernatant was removed and the fluorescence of the solution was examined with a Perkin-Elmer 650-40 Fluorescence Spectrophotometer in ratio mode. Excitation and emission wavelengths were 470 and 530 nm, respectively, and excitation and emission slits were at five and eight, respectively. The fluorescence of each spot was evaluated as a percentage of the total fluorescence of all spots in the lane.

Quantitative and Qualitative Fluorescence Microscopy

Diffusion and intercellular transport measurements were performed on an ACAS 570 Interactive Laser Cytometer (Meridian Instruments, Okemos, MI) as described in Baron-Epel et al. (1988) and Gharyal et al. (1989). This instrument was utilized to photobleach the cells, record

fluorescence redistribution as pseudocolor cellular images, and calculate fluorescence recovery curves. In brief, a typical experiment was performed in the following manner. Cells were placed on a slide that rested on an automated computer-controlled stage that moved the sample in 1.5-μm steps in a two-dimensional grid, past a microscope objective that focused the excitation beam (488 nm) from an argon-ion laser to a 1-μm diameter beam on the sample. Photobleaching occurred through the rapid bleaching of multiple points within a designated cell. A photomultiplier tube captured the emission intensities from each addressed point prior to (prebleach) and following (postbleach) photobleaching. The fluorescence intensity values were converted by computer into a color-coded image displayed on a cathode ray tube from which photographs were taken. Images were captured at 1.5-min intervals following photobleaching. In all photobleaching experiments, single cell controls were utilized to demonstrate that fluorescence recovery was not a result of a photoreactivation of the fluorescent probes. Confocal analyses of dye distribution were performed on an Insight Bilateral Scanning Confocal Microscope (Meridian Instruments), utilizing the 488-nm laser line from an air-cooled, argon-ion laser for excitation. Hard copy images from the confocal microscope were obtained by conventional 35-mm photography of the illuminated samples, using 400 ASA color film pushed to 800 ASA.

ACKNOWLEDGMENTS

This work was supported by a grant from the U.S.—Israel Binational Agriculture Research and Development Fund (Project No. US-1384-87). A special thanks to Ms. Linda Lang for superior secretarial assistance.

Received October 2, 1992; accepted November 18, 1992.

REFERENCES

Baron-Epel, O., Hernandez, D., Jiang, L.W., Meiners, S., and Schindler, M. (1988). Dynamic continuity of cytoplasmic and membrane compartments between plant cells. J. Cell Biol. **106,** 715–721.

Berridge, M.J. (1984). Inositol triphosphate and diacylglycerol as second messengers. Biochem. J. **220,** 345–360.

Dragsten, P.R., Blumenthal, R., and Handler, J.S. (1981). Membrane asymmetry in epithelia: Is the tight junction a barrier to diffusion in the plasma membrane? Nature **294,** 718–721.

Exton, J.H. (1990). Signaling through phosphatidylcholine breakdown. J. Biol. Chem. **265,** 1–3.

Farmer, E.E., Johnson, R.R., and Ryan, C.A. (1992). Regulation of expression of proteinase inhibitor genes by methyl jasmonate and jasmonic acid. Plant Physiol. **98,** 995–1002.

Gharyal, P.K., Ho, S-C., Wang, J.L., and Schindler, M. (1989). O-antigen from *Bradyrhizobium japonicum* lipopolysaccharide inhibits intercellular (symplast) communication between soybean (*Glycine max*) cells. J. Biol. Chem. **264,** 12119–12121.

Gundlach, H., Müller, M.J., Kutchan, T.M., and Zenk, H. (1992). Jasmonic acid is a signal transducer in elicitor-induced plant cell cultures. Proc. Natl. Acad. Sci. USA **89,** 2389–2393.

Hepler, P.K., Palevitz, B.A., Lancelle, S.A., McCauley, M.M., and Lichtschleidl, I. (1990). Cortical endoplasmic reticulum in plants. J. Cell Sci. **96,** 355–373.

Lipsky, N.G., and Pagano, R.E. (1985). Intracellular translocation of fluorescent sphingolipids in cultured fibroblasts: Endogenously synthesized sphingomyelin and glucosyl cerebroside analogs pass through the Golgi apparatus en route to the plasma membrane. J. Cell Biol. **100,** 27–34.

Lopez-Saez, J.F., Giménéz-Martin, G., and Risûeno, M. (1966). Fine structure of the plasmodesma. Protoplasma **61,** 81–84.

Metcalf, T.N., III, Wang, J.L., and Schindler, M. (1986). Lateral diffusion of phospholipids in the plasma membrane of soybean protoplasts: Evidence for membrane lipid domains. Proc. Natl. Acad. Sci. USA **83,** 95–99.

Metcalf, T.N., III, Wang, J.L., Schubert, K.R., and Schindler, M. (1983). Lectin receptors on the plasma membrane of soybean cells. Binding and lateral diffusion of lectins. Biochemistry **22,** 3969–3975.

Osborn, M.J., Gander, J.E., Parisi, E., and Carson, J. (1972). Mechanism of assembly of the outer membrane of *Salmonella typhimurium.* Isolation and characterization of cytoplasmic and outer membrane. J. Biol. Chem. **247,** 3962–3972.

Overall, R.L., Wolfe, J., and Gunning, B.E.S. (1982). Intercellular communication in Azolla roots. I. Ultrastructure of plasmodesmata. Protoplasma **111,** 134–150.

Pagano, R.E., and Longmuir, K.J. (1985). Phosphorylation, transbilayer movement and facilitated intracellular transport of diacylglycerol are involved in the uptake of a fluorescent analog of phosphatidic acid by cultured fibroblasts. J. Biol. Chem. **260,** 1909–1916.

Pelech, S.L., and Vance, P.E. (1989). Signal transduction via phosphatidylcholine cycles. Trends Biosci. **14,** 28–30.

Pfaffmann, H., Hartmann, E., Brightman, A.O., and James Morré, D. (1987). Phosphatidylinositol specific phospholipase C of plant stems. Plant Physiol. **85,** 1151–1155.

Quader, H., Hofmann, A., and Schnepf, E. (1989). Reorganization of the endoplasmic reticulum in epidermal cells of onion bulb scales after cold stress: Involvement of cytoskeletal elements. Planta **177,** 273–280.

Quader, H., and Schnepf, E. (1986). Endoplasmic reticulum and cytoplasmic streaming: Fluorescence microscopical observations in adaxial epidermis cells of onion bulb scales. Protoplasma **131,** 250–252.

Robards, A.W. (1968). A new interpretation of plasmodesmatal ultrastructure. Planta **82,** 200–218.

Robards, A.W. (1976). Plasmodesmata in higher plants. In Intercellular Communication in Plants: Studies on Plasmodesmata, B.E.S. Gunning and A.W. Robards, eds. (Berlin: Springer-Verlag), pp. 15–57.

Robards, A.W., and Lucas, W.J. (1990). Plasmodesmata. Annu. Rev. Plant Physiol. Plant Mol. Biol. **41,** 369–419.

Shotten, G. (1989). Confocal scanning optical microscopy and its applications for biological specimens. J. Cell Sci. **94,** 175–206.

Somerville, C., and Browse, J. (1991). Plant lipids: Metabolism, mutants, and membranes. Science **252,** 80–87.

Staehelin, L.A., and Chapman, R.L. (1987). Secretion and membrane recycling in plant cells: Novel intermediary structures visualized in ultrarapidly frozen sycamore and carrot suspension-culture cells. Planta **171,** 43–57.

Tate, B.F., Shaller, G.E., Sussman, M.R., and Crain, R.C. (1989). Characterization of a polyphosphoinositide phospholipase C from the plasma membrane of *Avena sativa.* Plant Physiol. **91,** 1275–1279.

Terasaki, M., and Reese, T.S. (1992). Characterization of endoplasmic reticulum by colocalization of BiP and dicarbocyanine dyes. J. Cell Sci. **101,** 315–322.

Terasaki, M., Song, J., Wong, J.R., Weiss, M.J., and Chen, L.B. (1984). Localization of endoplasmic reticulum in living and glutaraldehyde fixed cells with fluorescent dyes. Cell **38,** 101–108.

Tilney, L.G., Cooke, T.J., Connelly, P.S., and Tilney, M.S. (1991). The structure of plasmodesmata as revealed by plasmolysis, detergent extraction, and protease digestion. J. Cell Biol. **112,** 739–747.

Uster, P.S., and Pagano, R.E. (1986). Synthesis and properties of fluorescent analogs of cytidine diphosphate-diacylglycerol and phosphatidylinositol. In Enzymes of Lipid Metabolism II, L. Freysz, H. Dreyfus, R. Massarelli, and S. Gatt, eds, Nato ASI Series Vol. 116, (Heidelberg: Springer-Verlag), pp. 493–500.

Vance, J.E. (1990a). Phospholipid synthesis in a membrane fraction associated with mitochondria. J. Biol. Chem. **265,** 7248–7256.

Vance, J.E. (1990b). Newly made phosphatidylserine and phosphatidylethanolamine are preferentially translocated between rat liver mitochondria and endoplasmic reticulum. J. Biol. Chem. **266,** 89–97.